THE JOURNAL OF PHYSICAL CHEMISTRY Letters

Letter

Cite This: J. Phys. Chem. Lett. 2019, 10, 2538−2545

pubs.acs.org/JPCL

Excited-State Potential Energy Surfaces, Conical Intersections, and Analytical Gradients from Ground-State Density Functional Theory

Yuncai Mei[†] and Weitao Yang*[,†,‡]

[†]Department of Chemistry, Duke University, Durham, North Carolina 27708, United States

[‡]Key Laboratory of Theoretical Chemistry of Environment, School of Chemistry and Environment, South China Normal University, Guangzhou 510006, China

Supporting Information

ABSTRACT: Kohn−Sham density functional theory (KS-DFT) has been a well-established theoretical foundation for ground-state electronic structure and has achieved great success in practical calculations. Recently, utilizing the eigenvalues from KS or generalized KS (GKS) calculations as an approximation to the quasiparticle energies, our group demonstrated a method to calculate the excitation energies from (G)KS calculation on the ground-state $(N-1)$-electron system. This method is now called QE-DFT (quasiparticle energies from DFT). In this work, we extend this QE-DFT method to describe excited-state potential energy surfaces (PESs), conical intersections, and the analytical gradients of excited-state PESs. The analytical gradients were applied to perform geometry optimization for excited states. In conjunction with several commonly used density functional approximations, QE-DFT can yield PESs in the vicinity of the equilibrium structure with accuracy similar to that from time-dependent DFT (TD-DFT). Furthermore, it describes conical intersection well, in contrast to TD-DFT. Good results for geometry optimization, especially bond length, of low-lying excitations for 14 small molecules are presented. The capability of describing excited-state PESs, conical intersections, and analytical gradients from QE-DFT and its efficiency based on just ground-state DFT calculations should be of great interest for describing photochemical and photophysical processes in complex systems.

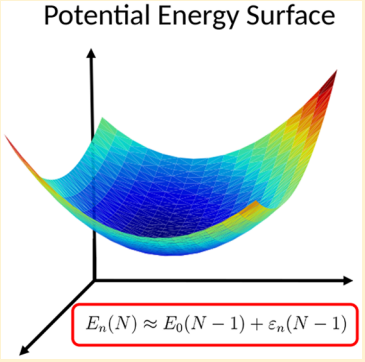

The excited-state potential energy surface (PES), the excited-state total energy as a function of geometrical structure, is an important property for describing photochemical and photophysical processes in chemistry, biology, and material science. Accurately describing the PES for the excited state provides critical information for many important problems, including excited-state geometry optimization that searches the excited-state PES for minimum and stationary points to obtain excited-state molecular structures, conical intersections,[1,2] and nonadiabatic dynamics.[3]

To obtain reliable excited-state PESs, many high-level methods can be applied to calculate the total energy of excited states with high accuracy, including the multireference configuration interaction (MRCI),[4,5] the complete active space second-order perturbation theory (CASPT2),[6,7] and equation-of-motion and linear response coupled-cluster theories (EOM-CC and LR-CC).[8−12] However, these methods are computationally demanding, which hinders their application to large systems in practice.

With broad applications to large and complex systems, Kohn−Sham density functional theory (KS-DFT) has a well-established theoretical foundation for electronic structure of ground states.[13−15] Because of its efficiency and accuracy, KS-DFT has achieved great success in practical calculations. For excited-state calculations, several methods have been developed extending the framework of KS-DFT. Time-dependent DFT (TD-DFT)[16,17] has been widely used to calculate excitation energies[18,19] and optimize geometries for excited states.[20,21] However, TD-DFT with commonly used density functional approximations (DFAs) still faces key challenges for excitations related to double excitations, charge transfer, and Rydberg states.[22−30] It also fails to describe the topology of PESs near conical intersections.[24] Besides TD-DFT, the Δ self-consistent field (ΔSCF) approach,[31,32] while not rigorously established as a theory, is another useful method, in which a non-Aufbau occupation is applied to an SCF procedure to describe excited states. In order to avoid the non-Aufbau electronic configuration from collapsing to the ground state within regular ΔSCF calculations, modifications to the SCF procedure, such as maximum overlap method (MOM)[33] and initial maximum overlap method (IMOM),[34] have been developed to overcome the issue, achieving good performance for calculating excitation energies, geometries of excited states, and conical intersections.[33−38] Other methods in the framework of ΔSCF that apply various constrains to obtain the excited states of interest have been reported to provide good excitation energies and capture conical intersections well, including constrained variational DFT (CV-DFT),[39,40] con-

Received: March 12, 2019
Accepted: April 30, 2019
Published: April 30, 2019

DOI: 10.1021/acs.jpclett.9b00712
J. Phys. Chem. Lett. 2019, 10, 2538−2545

strained DFT (CDFT),[41] orthogonality-constrained DFT,[42,43] and excited constrained DFT (XCDFT).[44]

In this work, we pursue a method that describes the excited-state PES directly from a ground-state KS or generalized KS (GKS) calculation by using the eigenvalues. Note that we use (G)KS eigenvalues to indicate orbital energies either from KS calculations for any approximate E_{xc} as an explicit and continuous functional of electron density (such as the local density approximation (LDA) and the generalized gradient approximation (GGA)) or from GKS calculations for any approximate E_{xc} as an explicit and continuous functional of the noninteracting one-particle density matrix (such as hybrid functionals). The use of KS or GKS in these two different types of functionals originates from the connection of its highest occupied molecular orbital (HOMO) and lowest unoccupied molecular orbital (LUMO) eigenvalue to the chemical potentials, as established by Cohen, Mori-Sanchez, and Yang.[45,46]

In ground-state DFT calculations, it has been rigorously shown that the frontier orbital eigenvalue of HOMO/LUMO is the corresponding chemical potential for electron removal/electron addition associated with the approximate functional used.[45,46] When the applied DFA has the minimum delocalization error,[47] the chemical potentials (HOMO and LUMO energies) approximate accurately the lowest ionization energy and highest electron affinity, which are the quasiparticle energies. This was demonstrated, for example, in the recently developed localized orbital scaling correction (LOSC) approach,[48] which provides a size-consistent elimination of the delocalization error. Beyond HOMO and LUMO energies, the remaining (G)KS eigenvalues are of considerable interest. With extensive numerical results, our group has shown in recent work that the remaining (G)KS orbital energies from a DFA with minimum delocalization error can also well approximate the corresponding quasiparticle energies;[49] that is, the occupied orbital energies lower than HOMO approximate higher ionization potentials (IPs) and unoccupied orbital energies higher than LUMO approximate lower electron affinities (EAs). The quaisparticle energy prediction from our method is comparable or better than that from the much more expensive many-body GW Green's function in extensive tests for 40 large molecular systems.[49] This observation indicates that different states (ground and excited states) of an N-electron system can be obtained from orbital energies of the ground-state $(N-1)$-electron system via a one-electron addition process.[49] Therefore, the excitation energy of an N-electron system can be calculated as the (G)KS orbital energy difference of the $(N-1)$-electron system with the same external potential.[49]

Furthermore, our previous work has shown that commonly used DFAs, such as LDAs, GGAs, and hybrid GGAs, can yield good low-lying excitation energies.[49] Although the orbital energies from these conventional DFAs can not approximate quasiparticle energies accurately because of the delocalization error,[50−52] the good performance of these DFAs for low-lying excitation energies was attributed to error cancellation within this method.[49] For Rydberg[49] and charge-transfer[53] excitations, conventional DFAs face challenges in providing reliable results. However, applying the recently developed localized orbital scaling correction (LOSC)[48] to these DFAs can greatly improve the results. We note that the Bartlett group also reported recently that applying the QTP (Quantum Theory Project) class of functionals including long-range Hartree−Fock exchange with the same methodology can yield good excitation energies for 10 simple test molecules.[54] We now call this method[49,54] QE-DFT, referring to quasiparticle energies from DFT. QE-DFT is the simplest approach to excitation energies and can provide good prediction of excitation energies from (G)KS orbital energies. In this Letter, we explore further the description of excited-state PESs and conical intersections with QE-DFT and we derive the analytical gradients of this method, which are needed for application in geometry optimization of excited states and nonadiabatic dynamics.

We first review the QE-DFT method to describe excited states via (G)KS orbital energies in ground-state calculations.[49,54] Starting from the ground state of the $(N-1)$-electron system, the particle part of the quasiparticle energy, $\omega_n^+(N-1)$, connects the ground state of the $(N-1)$-electron system, $E_0(N-1)$, to the nth excited state of the N-electron system, $E_n(N)$, via adding one electron to the unoccupied orbital. With observations that the unoccupied orbital energy $\varepsilon_n(N-1)$ approximates the quasiparticle energy, we have the following relation:

$$\varepsilon_n(N-1) \approx \omega_n^+(N-1) = E_n(N) - E_0(N-1) \tag{1}$$

When eq 1 is rearranged, $E_n(N)$, the excited-state energy of an N-electron system, can be approximated from the ground-state DFT calculation of the $(N-1)$-electron system via using its unoccupied orbital energy

$$\begin{aligned} E_n(N) &= E_0(N-1) + \omega_n^+(N-1) \\ &\approx E_0(N-1) + \varepsilon_n(N-1) = E_n^{\text{QE-DFT}}(N) \end{aligned} \tag{2}$$

There are two things that need to be clarified for the QE-DFT method (eq 2). First, it should be pointed out that the QE-DFT method captures the interaction between the added electron and the collective hole (exciton binding).[55] In the ground state of the $(N-1)$-electron system, the collective hole is created by removing one electron from the HOMO of the ground state of the N-electron system. When one electron is added to the virtual orbital of the $(N-1)$-electron system to retrieve excited states of the N-electron system, the collective hole will interact with the added electron, and the electron−hole interaction is thus captured by the particle part of the quasiparticle energy of the $(N-1)$-electron system. Second, the total energy from the QE-DFT method is not a self-consistent calculation for the N-electron system. Instead, it is only a self-consistent calculation for the $(N-1)$-electron system to obtain its total energy and eigenvalues. Because quasiparticle energies of the $(N-1)$-electron system are approximated by the (G)KS eigenvalues and the quasiparticle energy of the ground-state $(N-1)$-electron system, according to its definition, is related to an N-electron system by one electron addition process, the relation shown in eq 2 does not need any self-consistent calculation for the N-electron system.

Considering most $(N-1)$-electron systems are open shell cases (assuming one more α electron than β electron), adding one electron to a unoccupied orbital with α spin forms a triplet excited state, $E(\uparrow\uparrow)$, that can be used immediately. However, adding one electron to an unoccupied orbital with β spin forms a spin-mixed excited state, $E(\uparrow\downarrow)$. To describe singlet excited states within this method, we apply the commonly used spin purification process,[56] namely

$$E_{\text{singlet}} = 2E(\uparrow\downarrow) - E(\uparrow\uparrow) \tag{3}$$

DOI: 10.1021/acs.jpclett.9b00712
J. Phys. Chem. Lett. 2019, 10, 2538−2545

This spin purification process is effective to reduce the spin contamination and improve the results for excited states. It has been shown to improve the excitation energy results in ΔSCF calculations.[36] In addition, the recent work from our laboratory on applying GW approximation to calculate the quasiparticle energies of an $(N-1)$-electron system demonstrates that the same spin purification process can yield both excellent singlet and triplet excitation energies for low-lying and charge-transfer states for many molecules.[55] These results from the GW calculation[55] suggest that, as long as the quasiparticle energies are well-approximated by (G)KS eigenvalues, good performance on total energies of excited states, singlet−triplet splittings, and excitation energies can be obtained from QE-DFT.

Now considering the spin of orbitals and substituting eq 2 into eq 3, we can express the singlet excited-state energy from QE-DFT as the following:

$$E_{\text{singlet}}^{\text{QE-DFT}}(N) = E_0(N-1) + 2\varepsilon_{n\beta}(N-1) - \varepsilon_{n\alpha}(N-1) \tag{4}$$

With eqs 2 and 4, the excited-state energies for a molecule at different geometrical structures can be calculated from the ground-state DFT method. Therefore, the PESs of excited states can be obtained.

The analytical gradient of an N-electron system from the QE-DFT method involves two terms from the $(N-1)$-electron system calculation, namely, the gradient of the ground-state total energy of the $(N-1)$-electron system and the gradient of the corresponding orbital energy. Taking eq 2 as an example, the gradient with respect to nuclear coordinate $\mathbf{R}$ is expressed as

$$\nabla_{\mathbf{R}} E_n^{\text{QE-DFT}}(N) = \nabla_{\mathbf{R}} E_0(N-1) + \nabla_{\mathbf{R}} \varepsilon_n(N-1) \tag{5}$$

The gradient of total energy from DFT involves the Hellman−Feynman term (noted as G_1) and the Pulay term (noted as G_2), and it is given by[57−61]

$$\nabla_{\mathbf{R}} E_{\text{tot}} = G_1 + G_2 \tag{6}$$

The Hellman−Feynman term comes from the derivative of the exact Hamiltonian of the interacting system, and it is given by[57]

$$G_1 = \int \rho(\mathbf{r}) \nabla_{\mathbf{R}} v(\mathbf{r}, \mathbf{R}) \mathrm{d}\mathbf{r} + \nabla_{\mathbf{R}} E_{\text{nuc}}(\mathbf{R}) \tag{7}$$

where $v(\mathbf{r}, \mathbf{R})$ is the external potential and $E_{\text{nuc}}(\mathbf{R})$ is the nuclei interaction potential energy. The Pulay term comes from the derivative of the wave function with respect to nuclear coordinates $\mathbf{R}$, and it is given by[58,59]

$$G_2 = \sum_{i\sigma}^{\text{occ}} \langle \varphi'_{i\sigma} | h_s - \varepsilon_{i\sigma} | \varphi_{i\sigma} \rangle + \text{c.c.} \tag{8}$$

where h_s is the (G)KS Hamiltonian for the noninteracting system, σ the spin of electron, and $\varphi'_{i\sigma}$ derivative of molecular orbital $\varphi_{i\sigma}$ to nuclear coordinates with fixed coefficients $\{C_{i\mu}\}$ for the expansion of basis sets $\{\phi_\mu\}$, namely

$$\varphi'_{i\sigma} = \sum_{\mu} C_{i\mu} \nabla_{\mathbf{R}} \phi_\mu \tag{9}$$

As shown in eq 8, the Pulay term will vanish at the condition that the (G)KS equations are solved exactly with a complete basis set or with basis sets not dependent on nuclear coordinates, such as plane waves. However, when a finite number of atom-centered basis sets are used, the contribution from the Pulay term should be included. Substituting eqs 7 and 8 into eq 6, one can obtain the gradient of total energy from the (G)KS-DFT calculation. Clearly, this gradient of total energy can be directly used in our QE-DFT method with only the change of electron number from N to $N-1$.

The gradient of (G)KS orbital energy ε_n for the $(N-1)$-electron system can be expressed as the following:

$$\nabla_{\mathbf{R}} \varepsilon_n = \nabla_{\mathbf{R}} \langle \varphi_n | h_s | \varphi_n \rangle \tag{10}$$

$$= \langle \varphi_n | \nabla_{\mathbf{R}} h_s | \varphi_n \rangle + (\langle \nabla_{\mathbf{R}} \varphi_n | h_s | \varphi_n \rangle + \text{c.c.}) \tag{11}$$

Similarly to the gradient of total energy, the first term shown in eq 11 is similar to the Hellman−Feynman term that comes from the derivative of the (G)KS Hamiltonian h_s with respect to nuclear coordinates $\mathbf{R}$, and the second term is similar to the Pulay term that comes from the atomic basis set dependence on geometry. As shown in the second term of eq 11, the gradient of orbital energy involves the derivatives of molecular orbital coefficients with respect to nuclear coordinates. The direct approach to capture this contribution is solving the coupled-perturbed SCF equations,[62] which are dependent on nuclear coordinates and have $3N$ degrees of freedom (N being the number of atoms in the system). To reduce computational complexity, the Z vector method[63,64] that is independent of the nuclear coordinates is normally applied to reduce the degree of freedom by solving just one Z vector equation. The Z vector method has been commonly used in many calculations in which the first-order changes of molecular orbital coefficients are involved, such as energy gradient from CIS,[65] TD-HF,[66] and TD-DFT.[67] Here, the Z vector method is also applicable in calculation of energy gradients from the QE-DFT method. In the Supporting Information, we derive the explicit expression of the (G)KS orbital energy (eq 11) for implementation.

We now compare the computational cost between QE-DFT and the state-of-art TD-DFT method for excited-state calculations. For the total energy calculation of excited states, QE-DFT is computationally much more efficient than TD-DFT. Calculating many excitation energies involves only a ground-state (G)KS calculation on the $(N-1)$-electron system. In an iterative algorithm, the operational complexity of diagonalization of the Fock matrix in the (G)KS equation has a scaling of $O(N^2)$ (N being the dimension of the basis set). Moreover, because all the eigenvalues, used in QE-DFT to retrieve different excited state, are given from a single DFT calculation, QE-DFT is computationally much more efficient for describing many excited states at once. In constrast, TD-DFT, as a linear response theory from the ground-state DFT calculation, involves solving the TD-DFT equation with a dimension of $N_{\text{occ}}N_{\text{vir}} = O(N^2)$ (N_{occ} being the dimension of the occupied orbital space and N_{vir} being the dimension of the virtual orbital space).[68] Therefore, the scaling of solving the TD-DFT equation is $O(N^4)$. To achieve fast calculation in practice, the Davidson algorithm[69] is normally applied in TD-DFT to determine the lowest few eigenvalues, associated with low-lying excited states. In this way, calculating high excited states in TD-DFT would become increasingly expensive, because all the lower states have to be calculated as well.

For the analytical gradient calculation, QE-DFT should be computationally similar or cheaper than TD-DFT. There are two reasons: (1) Both methods need to solve the Z vector

DOI: 10.1021/acs.jpclett.9b00712
J. Phys. Chem. Lett. 2019, 10, 2538−2545

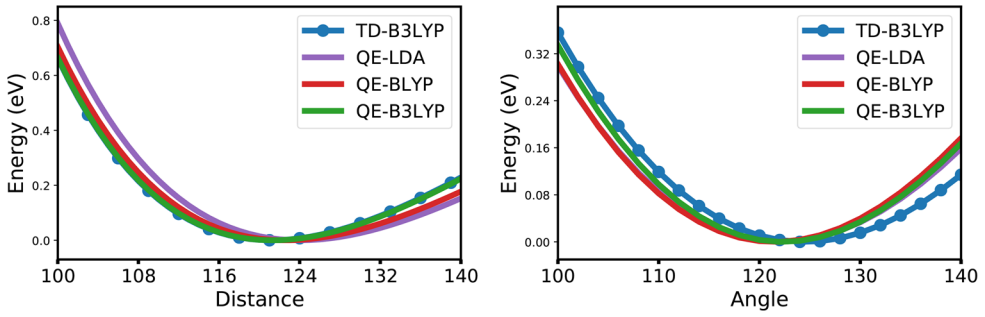

(a) BH (b) C_2H_2

Figure 1. Calculated PESs of excited states for two molecules in the vicinity of their equilibrium structures: (a) $^1\Pi$ state of BH and (b) ^1A_u state of C_2H_2. The energy of each PES is relative to its minimum value. The PES of BH is plotted with respect to B−H bond length in picometers. The PES of C_2H_2 is plotted with respect to the ∠HCC bond angle in degrees. The H−C and C−C bond length in C_2H_2 are fixed at 110 and 132 pm, respectively. 6-311+g* is used as the basis set for QE-DFT calculations. TD-DFT calculations are conducted from the Gaussian 09 package,[76] and 6-311+g** is used as the basis set.

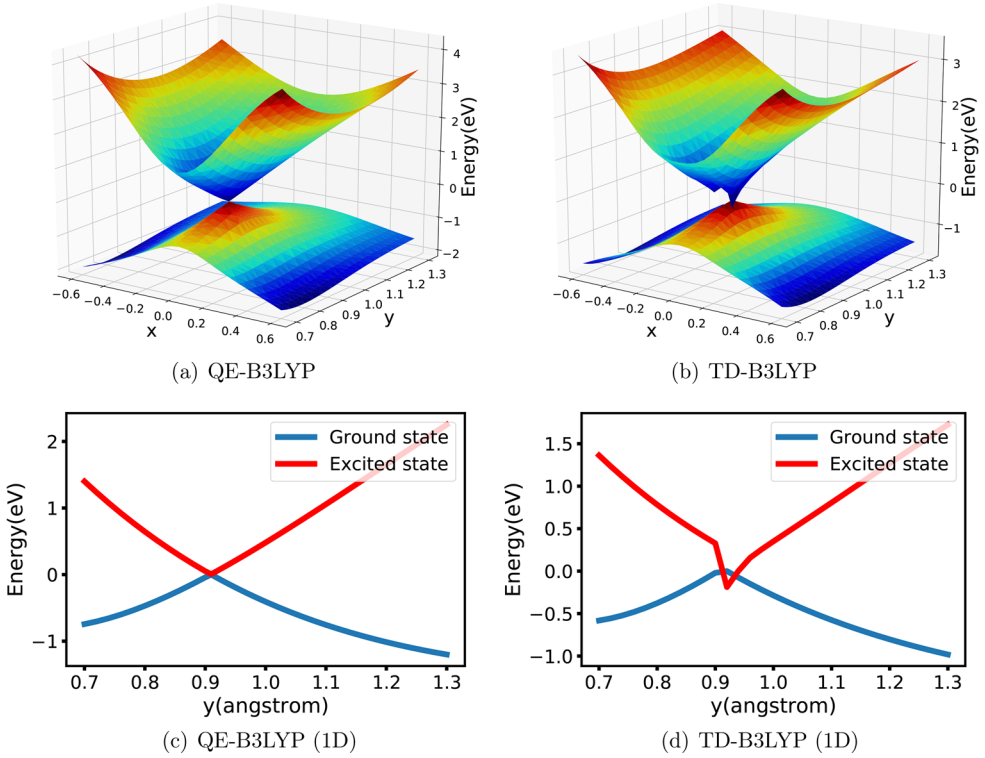

(a) QE-B3LYP (b) TD-B3LYP

(c) QE-B3LYP (1D) (d) TD-B3LYP (1D)

Figure 2. Calculated conical intersection and PES of the ground and first excited states for H_3 molecule. cc-pVTZ is used as the basis set. The potential energy is relative to the maximum energy in the ground-state PES. With fixing two H atoms at positions (0.525, 0) and (−0.525, 0) in the Cartesian coordinates system, the potential energy is given as a function of coordinates of the third H atom (x, y). The PESs from QE-B3LYP and TD-B3LYP are plotted in panels a and b, respectively. One-dimensional potential energy curves from (c) QE-B3LYP and (d) TD-B3LYP are obtained by slicing the PES along the y-axis with x fixed at 0.0.

equation, which is of dimension of $N_{occ}N_{vir}$ (QE-DFT; see the Supporting Information, TD-DFT; see ref 21), which means the computational scalings of QE-DFT and TD-DFT are similar. (2) All the matrix elements needed in QE-DFT for analytical gradient are needed in the TD-DFT calculation as well, with no more effort required from QE-DFT than TD-DFT. Thus, based on the foregoing analysis, our QE-DFT method is a computationally similar or cheaper method than TD-DFT for calculating analytical gradients of excited states.

To test the performance of QE-DFT, we implemented QE-DFT in our in-house program, QM4D package,[70] to conduct all the calculations. For geometry optimization, we choose 14 small molecules (BF, BH, C_2H_2, CO, CH_2O, CH_2S, HCN, HCP, Li_2, N_2, SiO, t-$(CHO)_2$, SiF_2, and CCl_2) from the test set that was used by Furche et al.[20,21] and Besley et al.[35] in examining the performance of TD-DFT and ΔSCF for excited-state properties. We include only the lowest singlet excitations (HOMO to LUMO excitation), which are available from experimental references for comparison. These test cases range from diatomic molecules to polyatomic molecules. Their structural parameters of excited states, including bond length, bond angle, and dihedral angles, are compared with experimental references and the calculated results from TD-DFT and ΔSCF. Because the $(N-1)$-electron system of all these molecules are open-shell systems, we used unrestricted calculations. The applied basis set is 6-311+g*, which is close

DOI: 10.1021/acs.jpclett.9b00712
J. Phys. Chem. Lett. 2019, 10, 2538−2545

Table 1. Geometry Optimization Results of Excited States from Different Methods Compared with Experiment[a]

Molecule	State		Exp[b]	TD-B3LYP[b]	Δ-B3LYP[b]	QE-LDA	QE-BLYP	QE-B3LYP
BF	$1^1\Pi$	B-F	130	131	132	131	134	133
BH	$1^1\Pi$	B-H	122	121	121	124	123	121
C_2H_2	1^1A_u	C-C	139	137	137	133	137	131
		∠HCC	120	122	122	126	125	130
CO	$1^1\Pi$	C-O	124	123	122	121	124	122
CH_2O	$1^1A''$	C-H	110	110	110	110	109	108
		C-O	132	129	132	129	133	134
		∠HCH	118	117	117	111	113	114
		dihedral	34	44	38	50	49	49
CH_2S	1^1A_2	C-H	108	108	108	109	109	108
		C-S	168	169	171	169	175	194
		∠HCH	121	120	120	119	117	115
		dihedral	12	0	0	16	36	55
HCN	$1^1A''$	C-H	114	112	113	115	117	118
		N-C	130	130	130	126	129	129
		∠HCN	125	123	122	104	92	85
HCP	$1^1A''$	P-C	169	170	171	177	176	173
		∠HCP	128	130	128	131	131	87
Li_2	$1^1\Sigma_u^+$	Li-Li	311	303	304	318	293	297
N_2	$1^1\Sigma_u^-$	N-N	128	128	128	120	122	121
SiO	$1^1\Pi$	Si-O	162	162	164	162	166	172
CCl_2	1^1B_1	C-Cl	165	166	168	165	169	166
		∠ClCCl	131	138	130	130	129	130
SiF_2	1^1B_1	SiF	160	166	165	165	169	166
		∠FSiF	116	113	114	116	114	114
t-$(CHO)_2$	1^1A_u	C-H	112	110	110	111	110	109
		C-O	125	123	123	123	125	123
		C-C	146	148	149	145	147	147
		∠HCC	114	114	114	114	115	114
		∠OCC	124	125	125	125	125	125
Bond length								
MAE				2	2	3	4	5
MSE				-1	0	-1	0	0
MXE				8	7	8	18	26
Bond angle								
MAE				2	1	5	7	15
MSE				2	0	-2	-4	-12
MXE				7	3	21	33	41

[a]Bond length are in picometers, and angles are in degrees. Numbers marked red show large deviation to the experimental reference. [b]Data were taken from ref 35.

to the basis set used in Besley's work.[35] For DFT calculations, we applied only three conventional DFAs (LDA,[71,72] BLYP,[73,74] and B3LYP[73−75]) to perform geometry optimization at present, because implementation of solving coupled-perturbed SCF equations for orbital energy derivatives is straightforward for these conventional DFAs. Implementing the gradients of other special DFAs needs more effort, and their performance will be studied in future work. For example, our recently developed functional, LOSC-DFAs, has been shown to yield orbital energies that are much more accurate than those of conventional DFAs.[48,49] However, taking gradients of the corrected orbital energies from LOSC-DFAs will involve a set of localized orbitals (called orbitalets),[48] which will be carried out in future work.

We now present our results on the description of excited-state PESs. In Figure 1, the shapes of PES in the vicinity of equilibrium structures for two simple molecules, a linear molecule BH and a bent molecule C_2H_2 in their first singlet excited states, are plotted via eq 4 and compared with the calculated results from TD-DFT. Although the orbital energies from conventional DFAs deviate much from quasiparticle energies,[49] which may lead to error in the shape of PESs for describing excited states within the QE-DFT method, results of test molecules in Figure 1 show that excited-state PESs from QE-DFT are smooth and their shapes are similar to the ones from TD-DFT. This observation shows that the systematic delocalization errors for orbital energies from conventional DFAs are similar even at different geometrical structures for low-lying excited states and that the error cancellation is effective here. This extends the previous conclusion on the good accuracy and insensitivity of QE-DFT on the delocalization error of DFAs for low-lying excitation energies[49] to their potential energy surfaces. Such observation suggests that these conventional DFAs would still be applicable for describing low-lying excited-state PESs within QE-DFT.

Furthermore, we test QE-DFT to describe the PES with the more challenging conical intersection problem, for which TD-DFT with adiabatic approximation fails. Here we choose a well-studied case, the H_3 molecule.[77] It is known that ground-state and the first excited-state PESs for H_3 will intersect at one point at equilateral triangle geometry with D_{3h} symmetry. Fixing two H atoms on the *x*-axis at coordinates (0.525, 0) and (−0.525, 0) in a Cartesian coordinates system, we scan the PES by varying coordinates of a third H atom in the *xy*-plane. Panels a and b of Figure 2 show the calculated PESs from QE-B3LYP and TD-B3LYP respectively. According to these two figures, the topology of the conical intersection for H_3 can be well captured by QE-DFT, while TD-DFT fails with the surface collapsing around the conical intersection. Such different performances for QE-DFT and TD-DFT can further

DOI: 10.1021/acs.jpclett.9b00712
J. Phys. Chem. Lett. 2019, 10, 2538−2545

be observed from Figure 2c and 2d, in which a potential energy curve with $x = 0.0$ is plotted along the y-axis.

With the success of describing PESs for excited states, we continue to verify the results of optimized excited-state geometries. Table 1 summaries the optimized geometry parameters of the first singlet excited states for the test set. According to Table 1, QE-DFT shows good results for bond lengths. Even with the LDA functional, the mean absolute error (MAE) for the optimized bond length is 3 pm, which is close to the accuracy from TD-DFT and ΔSCF (1−2 pm). For the results from QE-BLYP and QE-B3LYP, the results are slightly worse with MAE up to 5 pm. Such an increase of MAE for QE-BLYP and QE-B3LYP can be attributed to several challenging cases with high absolute error over 10 pm (marked in red in Table 1). For other cases, there is no significant difference in the performance of test DFAs. In addition, the mean signed error (MSE) for bond length results are close to zero, indicating no significant bias from this method. For the prediction of bond angle, TD-DFT and ΔSCF show good results, with MAE being 2° and 1° and maximum absolute deviation (MXE) being 7° and 3°, respectively. The MAE for the results from QE-DFT (5−15° error) is larger than that for TD-DFT and ΔSCF because of a specific case, the HCN molecule, whose absolute error is larger than 20°. However, for bond angles from the remaining test cases, results from QE-DFT are close to the experimental reference. We believe these results for the challenging cases are related to inaccurate orbital energies from applied conventional DFAs. With application of better DFAs to yield more reliable orbital energies, improvements for these cases should be expected.

In conclusion, we demonstrate that the QE-DFT can describe excited-state PESs and conical intersections from a ground-state DFT calculation. With application of several commonly used DFAs, we observe that QE-DFT performs similarly to TD-DFT for describing excited-state PES in the vicinity of the equilibrium structure. In addition, QE-DFT can capture the conical intersection well, while TD-DFT encounters difficulty. We also developed the analytical gradient needed to perform excited-state geometry optimization and excited-state dynamics within the QE-DFT method and showed its good performance on geometry optimization, especially bond length, for 14 small test molecules. Considering the capability of describing excited-state PES, conical intersections, and gradients in this method and its efficiency based on just ground-state DFT calculations, we believe QE-DFT should be of great interest for describing photochemical and photophysical processes in complex systems.

■ ASSOCIATED CONTENT

Supporting Information

The Supporting Information is available free of charge on the ACS Publications website at DOI: 10.1021/acs.jpclett.9b00712.

Analytical expression for the gradient of (G)KS orbital energies and numerical verification of the analytical gradient (PDF)

■ AUTHOR INFORMATION

Corresponding Author

*E-mail: weitao.yang@duke.edu.

ORCID

Weitao Yang: 0000-0001-5576-2828

Notes

The authors declare no competing financial interest.

■ ACKNOWLEDGMENTS

The authors acknowledge support from the National Institutes of Health (Grant No. R01 GM061870-13) (W.Y.) and the Center for Computational Design of Functional Layered Materials (Award DE-SC0012575), an Energy Frontier Research Center funded by the US Department of Energy, Office of Science, Basic Energy Sciences (Y.M.).

■ REFERENCES

(1) Yarkony, D. R. Diabolical Conical Intersections. *Rev. Mod. Phys.* **1996**, *68*, 985−1013.
(2) Yarkony, D. R. Conical Intersections: The New Conventional Wisdom. *J. Phys. Chem. A* **2001**, *105*, 6277−6293.
(3) Tully, J. C. Perspective: Nonadiabatic Dynamics Theory. *J. Chem. Phys.* **2012**, *137*, 22A301.
(4) Helgaker, T.; Jorgensen, P.; Olsen, J. *Molecular Electronic-Structure Theory* ; John Wiley & Sons, 2014.
(5) Buenker, R. J.; Peyerimhoff, S. D. CI Method for the Study of General Molecular Potentials. *Theoret. Chim. Acta* **1968**, *12*, 183−199.
(6) Andersson, K.; Malmqvist, P. A.; Roos, B. O.; Sadlej, A. J.; Wolinski, K. Second-Order Perturbation Theory with a CASSCF Reference Function. *J. Phys. Chem.* **1990**, *94*, 5483−5488.
(7) Andersson, K.; Malmqvist, P.-A.; Roos, B. O. Second-order Perturbation Theory with a Complete Active Space Self-consistent Field Reference Function. *J. Chem. Phys.* **1992**, *96*, 1218−1226.
(8) Mukherjee, D.; Mukherjee, P. K. A Response-Function Approach to the Direct Calculation of the Transition-Energy in a Multiple-Cluster Expansion Formalism. *Chem. Phys.* **1979**, *39*, 325−335.
(9) ROWE, D. J. Equations-of-Motion Method and the Extended Shell Model. *Rev. Mod. Phys.* **1968**, *40*, 153−166.
(10) Sekino, H.; Bartlett, R. J. A Linear Response, Coupled-Cluster Theory for Excitation Energy. *Int. J. Quantum Chem.* **1984**, *26*, 255−265.
(11) Dalgaard, E.; Monkhorst, H. J. Some Aspects of the Time-Dependent Coupled-Cluster Approach to Dynamic Response Functions. *Phys. Rev. A: At., Mol., Opt. Phys.* **1983**, *28*, 1217−1222.
(12) Koch, H.; Jo/rgensen, P. Coupled Cluster Response Functions. *J. Chem. Phys.* **1990**, *93*, 3333−3344.
(13) Hohenberg, P.; Kohn, W. Inhomogeneous Electron Gas. *Phys. Rev.* **1964**, *136*, B864−B871.
(14) Kohn, W.; Sham, L. J. Self-Consistent Equations Including Exchange and Correlation Effects. *Phys. Rev.* **1965**, *140*, A1133−A1138.
(15) Parr, R. G.; Yang, W. *Density-Functional Theory of Atoms and Molecules*; International Series of Monographs on Chemistry; Oxford University Press: Oxford, 1994.
(16) Runge, E.; Gross, E. K. U. Density-Functional Theory for Time-Dependent Systems. *Phys. Rev. Lett.* **1984**, *52*, 997−1000.
(17) Gross, E. K. U.; Kohn, W. Local Density-Functional Theory of Frequency-Dependent Linear Response. *Phys. Rev. Lett.* **1985**, *55*, 2850−2852.
(18) Dreuw, A.; Head-Gordon, M. Single-Reference Ab Initio Methods for the Calculation of Excited States of Large Molecules. *Chem. Rev.* **2005**, *105*, 4009−4037.
(19) Laurent, A. D.; Jacquemin, D. TD-DFT Benchmarks: A Review. *Int. J. Quantum Chem.* **2013**, *113*, 2019−2039.
(20) Rappoport, D.; Furche, F. Analytical Time-Dependent Density Functional Derivative Methods within the RI-J Approximation, an Approach to Excited States of Large Molecules. *J. Chem. Phys.* **2005**, *122*, No. 064105.

DOI: 10.1021/acs.jpclett.9b00712
J. Phys. Chem. Lett. 2019, 10, 2538−2545

(21) Furche, F.; Ahlrichs, R. Adiabatic Time-Dependent Density Functional Methods for Excited State Properties. *J. Chem. Phys.* **2002**, *117*, 7433−7447.
(22) Tozer, D. J.; Handy, N. C. On the Determination of Excitation Energies Using Density Functional Theory. *Phys. Chem. Chem. Phys.* **2000**, *2*, 2117−2121.
(23) Maitra, N. T.; Zhang, F.; Cave, R. J.; Burke, K. Double Excitations within Time-Dependent Density Functional Theory Linear Response. *J. Chem. Phys.* **2004**, *120*, 5932−5937.
(24) Levine, B. G.; Ko, C.; Quenneville, J.; MartÍnez, T. J. Conical Intersections and Double Excitations in Time-Dependent Density Functional Theory. *Mol. Phys.* **2006**, *104*, 1039−1051.
(25) Casida, M. E.; Jamorski, C.; Casida, K. C.; Salahub, D. R. Molecular Excitation Energies to High-Lying Bound States from Time-Dependent Density- Functional Response Theory: Characterization and Correction of the Time-Dependent Local Density Approximation Ionization Threshold. *J. Chem. Phys.* **1998**, *108*, 4439−4449.
(26) Casida, M. E.; Salahub, D. R. Asymptotic Correction Approach to Improving Approximate Exchange−Correlation Potentials: Time-Dependent Density-Functional Theory Calculations of Molecular Excitation Spectra. *J. Chem. Phys.* **2000**, *113*, 8918−8935.
(27) TOZER, D. J.; HANDY, N. C. The Importance of the Asymptotic Exchange-Correlation Potential in Density Functional Theory. *Mol. Phys.* **2003**, *101*, 2669−2675.
(28) Tozer, D. J.; Handy, N. C. Improving Virtual Kohn−Sham Orbitals and Eigenvalues: Application to Excitation Energies and Static Polarizabilities. *J. Chem. Phys.* **1998**, *109*, 10180−10189.
(29) Dreuw, A.; Weisman, J. L.; Head-Gordon, M. Long-Range Charge-Transfer Excited States in Time-Dependent Density Functional Theory Require Non-Local Exchange. *J. Chem. Phys.* **2003**, *119*, 2943−2946.
(30) Dreuw, A.; Head-Gordon, M. Failure of Time-Dependent Density Functional Theory for Long-Range Charge-Transfer Excited States: The Zincbacteriochlorin-Bacteriochlorin and Bacteriochlorophyll-Spheroidene Complexes. *J. Am. Chem. Soc.* **2004**, *126*, 4007−4016.
(31) Ziegler, T.; Rauk, A.; Baerends, E. J. On the Calculation of Multiplet Energies by the Hartree-Fock-Slater Method. *Theoret. Chim. Acta* **1977**, *43*, 261−271.
(32) Jones, R. O.; Gunnarsson, O. The Density Functional Formalism, Its Applications and Prospects. *Rev. Mod. Phys.* **1989**, *61*, 689−746.
(33) Gilbert, A. T. B.; Besley, N. A.; Gill, P. M. W. Self-Consistent Field Calculations of Excited States Using the Maximum Overlap Method (MOM). *J. Phys. Chem. A* **2008**, *112*, 13164−13171.
(34) Barca, G. M. J.; Gilbert, A. T. B.; Gill, P. M. W. Simple Models for Difficult Electronic Excitations. *J. Chem. Theory Comput.* **2018**, *14*, 1501−1509.
(35) Hanson-Heine, M. W. D.; George, M. W.; Besley, N. A. Calculating Excited State Properties Using Kohn-Sham Density Functional Theory. *J. Chem. Phys.* **2013**, *138*, No. 064101.
(36) Kowalczyk, T.; Yost, S. R.; Voorhis, T. V. Assessment of the ΔSCF Density Functional Theory Approach for Electronic Excitations in Organic Dyes. *J. Chem. Phys.* **2011**, *134*, No. 054128.
(37) Terranova, U.; Bowler, D. R. Δ Self-Consistent Field Method for Natural Anthocyanidin Dyes. *J. Chem. Theory Comput.* **2013**, *9*, 3181−3188.
(38) Maurer, R. J.; Reuter, K. Assessing Computationally Efficient Isomerization Dynamics: ΔSCF Density-Functional Theory Study of Azobenzene Molecular Switching. *J. Chem. Phys.* **2011**, *135*, 224303.
(39) Ziegler, T.; Seth, M.; Krykunov, M.; Autschbach, J.; Wang, F. On the Relation between Time-Dependent and Variational Density Functional Theory Approaches for the Determination of Excitation Energies and Transition Moments. *J. Chem. Phys.* **2009**, *130*, 154102.
(40) Ziegler, T.; Krykunov, M.; Cullen, J. The Implementation of a Self-Consistent Constricted Variational Density Functional Theory for the Description of Excited States. *J. Chem. Phys.* **2012**, *136*, 124107.
(41) Kaduk, B.; Kowalczyk, T.; Van Voorhis, T. Constrained Density Functional Theory. *Chem. Rev.* **2012**, *112*, 321−370.
(42) Evangelista, F. A.; Shushkov, P.; Tully, J. C. Orthogonality Constrained Density Functional Theory for Electronic Excited States. *J. Phys. Chem. A* **2013**, *117*, 7378−7392.
(43) Verma, P.; Derricotte, W. D.; Evangelista, F. A. Predicting Near Edge X-Ray Absorption Spectra with the Spin-Free Exact-Two-Component Hamiltonian and Orthogonality Constrained Density Functional Theory. *J. Chem. Theory Comput.* **2016**, *12*, 144−156.
(44) Ramos, P.; Pavanello, M. Low-Lying Excited States by Constrained DFT. *J. Chem. Phys.* **2018**, *148*, 144103.
(45) Cohen, A. J.; Mori-Sánchez, P.; Yang, W. Fractional Charge Perspective on the Band Gap in Density-Functional Theory. *Phys. Rev. B: Condens. Matter Mater. Phys.* **2008**, *77*, 115123.
(46) Yang, W.; Cohen, A. J.; Mori-Sánchez, P. Derivative Discontinuity, Bandgap and Lowest Unoccupied Molecular Orbital in Density Functional Theory. *J. Chem. Phys.* **2012**, *136*, 204111.
(47) Mori-Sánchez, P.; Cohen, A. J.; Yang, W. Localization and Delocalization Errors in Density Functional Theory and Implications for Band-Gap Prediction. *Phys. Rev. Lett.* **2008**, *100*, 146401.
(48) Li, C.; Zheng, X.; Su, N. Q.; Yang, W. Localized Orbital Scaling Correction for Systematic Elimination of Delocalization Error in Density Functional Approximations. *Natl. Sci. Rev.* **2018**, *5*, 203−215.
(49) Mei, Y.; Li, C.; Su, N. Q.; Yang, W. Approximating Quasiparticle and Excitation Energies from Ground State Generalized Kohn-Sham Calculations. *J. Phys. Chem. A* **2019**, *123*, 666−673.
(50) Mori-Sánchez, P.; Cohen, A. J.; Yang, W. Localization and Delocalization Errors in Density Functional Theory and Implications for Band-Gap Prediction. *Phys. Rev. Lett.* **2008**, *100*, 146401.
(51) Cohen, A. J.; Mori-Sánchez, P.; Yang, W. Challenges for Density Functional Theory. *Chem. Rev.* **2012**, *112*, 289−320.
(52) Cohen, A. J.; Mori-Sánchez, P.; Yang, W. Insights into Current Limitations of Density Functional Theory. *Science* **2008**, *321*, 792−794.
(53) Mei, Y.; Yang, W. Charge Transfer Excitation Energies from Ground State Density Functional Theory Calculations. *J. Chem. Phys.* **2019**, *150*, 144109.
(54) Haiduke, R. L. A.; Bartlett, R. J. Communication: Can Excitation Energies Be Obtained from Orbital Energies in a Correlated Orbital Theory? *J. Chem. Phys.* **2018**, *149*, 131101.
(55) Jin, Y.; Yang, W. Excitation Energies from the Single-Particle Green's Function with the GW Approximation. *J. Phys. Chem. A* **2019**, *123*, 3199−3204.
(56) Ziegler, T.; Rauk, A.; Baerends, E. J. On the Calculation of Multiplet Energies by the Hartree-Fock-Slater Method. *Theoret. Chim. Acta* **1977**, *43*, 261−271.
(57) Delley, B. Analytic Energy Derivatives in the Numerical Local-density-functional Approach. *J. Chem. Phys.* **1991**, *94*, 7245−7250.
(58) Pulay, P. *Ab Initio* Calculation of Force Constants and Equilibrium Geometries in Polyatomic Molecules. I. Theory. *Mol. Phys.* **1969**, *17*, 197−204.
(59) Satoko, C. Direct Force Calculation in the Xα Method and Its Application to Chemisorption of an Oxygen Atom on the Al(111) Surface. *Chem. Phys. Lett.* **1981**, *83*, 111−115.
(60) Pople, J. A.; Gill, P. M.; Johnson, B. G. Kohn—Sham Density-Functional Theory within a Finite Basis Set. *Chem. Phys. Lett.* **1992**, *199*, 557−560.
(61) Johnson, B. G.; Gill, P. M. W.; Pople, J. A. The Performance of a Family of Density Functional Methods. *J. Chem. Phys.* **1993**, *98*, 5612−5626.
(62) Gerratt, J.; Mills, I. M. Force Constants and Dipole-Moment Derivatives of Molecules from Perturbed Hartree−Fock Calculations. I. *J. Chem. Phys.* **1968**, *49*, 1719−1729.
(63) Handy, N. C.; Schaefer, H. F. On the Evaluation of Analytic Energy Derivatives for Correlated Wave Functions. *J. Chem. Phys.* **1984**, *81*, 5031−5033.
(64) Schaefer, H. F., III; Goddard, J D.; Osamura, Y.; Yamaguchi, Y. *A New Dimension to Quantum Chemistry: Analytic Derivative Methods*

DOI: 10.1021/acs.jpclett.9b00712
J. Phys. Chem. Lett. 2019, 10, 2538−2545

in Ab Initio Molecular Electronic Structure Theory; Oxford University Press, 1994.
(65) Foresman, J. B.; Head-Gordon, M.; Pople, J. A.; Frisch, M. J. Toward a Systematic Molecular Orbital Theory for Excited States. *J. Phys. Chem.* **1992**, *96*, 135−149.
(66) Ortiz, J. V. One-electron Density Matrices and Energy Gradients in the Random Phase Approximation. *J. Chem. Phys.* **1994**, *101*, 6743−6749.
(67) Van Caillie, C.; Amos, R. D. Geometric Derivatives of Excitation Energies Using SCF and DFT. *Chem. Phys. Lett.* **1999**, *308*, 249−255.
(68) Stratmann, R. E.; Scuseria, G. E.; Frisch, M. J. An Efficient Implementation of Time-Dependent Density-Functional Theory for the Calculation of Excitation Energies of Large Molecules. *J. Chem. Phys.* **1998**, *109*, 8218−8224.
(69) Davidson, E. R. The Iterative Calculation of a Few of the Lowest Eigenvalues and Corresponding Eigenvectors of Large Real-Symmetric Matrices. *J. Comput. Phys.* **1975**, *17*, 87−94.
(70) An In-House Program for QM/MM Simulations. https://qm4d.org/.
(71) Slater, J. C. *The Self-Consistent Field for Molecules and Solids* ; McGraw-Hill, 1974.
(72) Vosko, S. H.; Wilk, L.; Nusair, M. Accurate Spin-Dependent Electron Liquid Correlation Energies for Local Spin Density Calculations: A Critical Analysis. *Can. J. Phys.* **1980**, *58*, 1200−1211.
(73) Becke, A. D. Density-Functional Exchange-Energy Approximation with Correct Asymptotic Behavior. *Phys. Rev. A: At., Mol., Opt. Phys.* **1988**, *38*, 3098−3100.
(74) Lee, C.; Yang, W.; Parr, R. G. Development of the Colle-Salvetti Correlation-Energy Formula into a Functional of the Electron Density. *Phys. Rev. B: Condens. Matter Mater. Phys.* **1988**, *37*, 785−789.
(75) Becke, A. D. Density-functional Thermochemistry. III. The Role of Exact Exchange. *J. Chem. Phys.* **1993**, *98*, 5648−5652.
(76) Frisch, M. J.; Trucks, G. W.; Schlegel, H. B.; Scuseria, G. E.; Robb, M. A.; Cheeseman, J. R.; Scalmani, G.; Barone, V.; Petersson, G. A.; Nakatsuji, H. et al. *Gaussian 09*, revision D.01; Gaussian, Inc., Wallingford CT, 2016.
(77) Halász, G.; Vibók, A.; Mebel, A. M.; Baer, M. A Survey of *Ab Initio* Conical Intersections for the H+H2 System. *J. Chem. Phys.* **2003**, *118*, 3052−3064.

DOI: 10.1021/acs.jpclett.9b00712
J. Phys. Chem. Lett. 2019, 10, 2538−2545